

Probing Conformational Hotspots For The Recognition And Intervention Of Protein Complex By Lysine Reactivity Profiling

Zheyi Liu,^{1*} Wenxiang Zhang,^{1,2*} Binwen Sun,^{1,3} Yaolu Ma,^{1,3} Min He,^{1,3} Yuanjiang Pan,² Fangjun Wang,^{1,3†}

¹CAS Key Laboratory of Separation Sciences for Analytical Chemistry, Dalian Institute of Chemical Physics, Chinese Academy of Sciences, Dalian 116023, China.

²Department of Chemistry, Zhejiang University, Hangzhou 310027, China.

³University of Chinese Academy of Sciences, Beijing 100049, China.

†Corresponding Author. E-mail: wangfj@dicp.ac.cn

*These authors contributed equally to this work.

*Corresponding Author. E-mail: wangfj@dicp.ac.cn

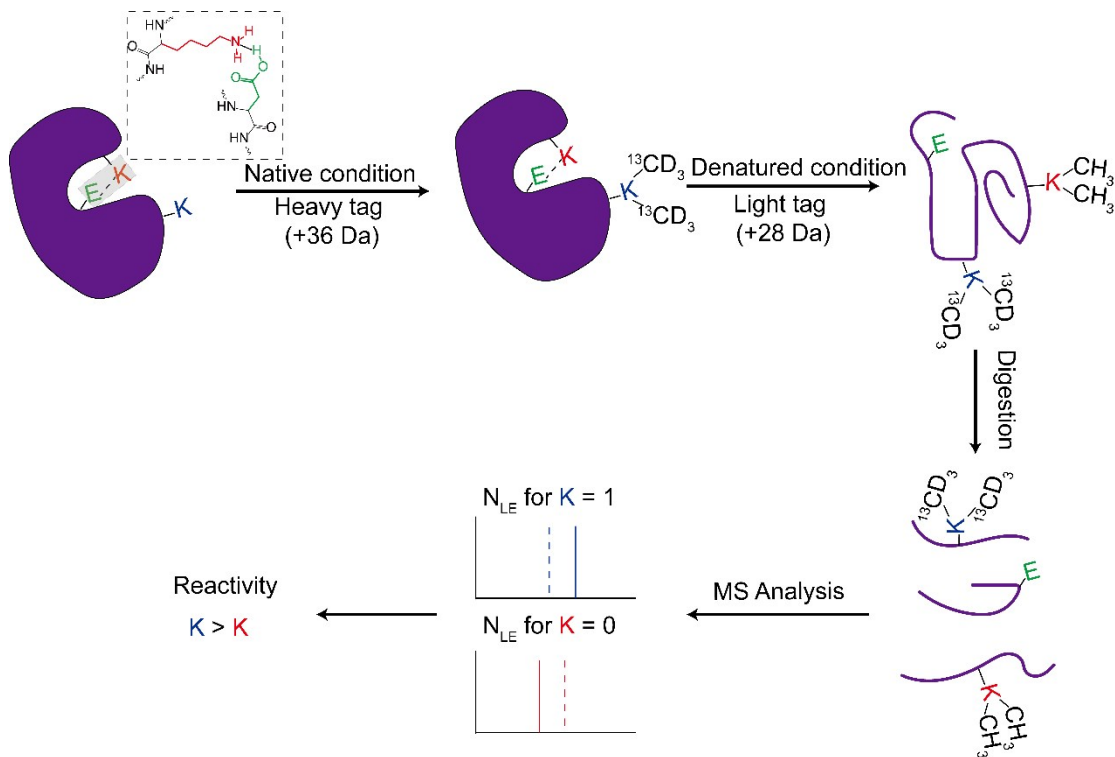


Fig. S1. The workflow of two-step isotope labeling-lysine reactivity profiling strategy. The first-step labeling is performed under native state with heavy isotope dimethyl tags. After denaturation, the second-step labeling is performed to completely labeled all of the lysine residues with light dimethyl tags.

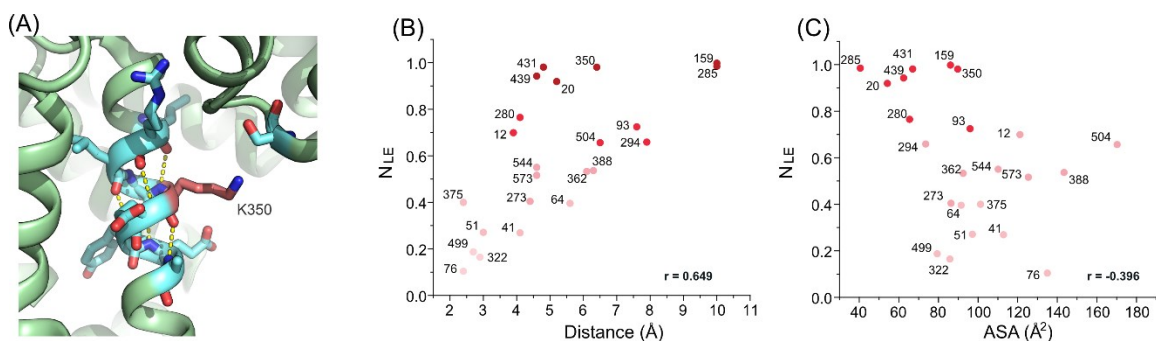


Fig. S2. Quantification of the relative lysine reactivities (N_{LE}) of purified BSA under native aqueous solution by TILLRP strategy. (A) The microenvironment of Lys³⁵⁰; (B) The correlation between the lysine N_{LE} values and the distances between lysine residues and their proximal acidic residues (the correlation coefficient r is 0.649); (C) The correlation between the lysine N_{LE} values and the corresponding solvent-accessible surface areas (SASAs) (the correlation coefficient r is -0.396).

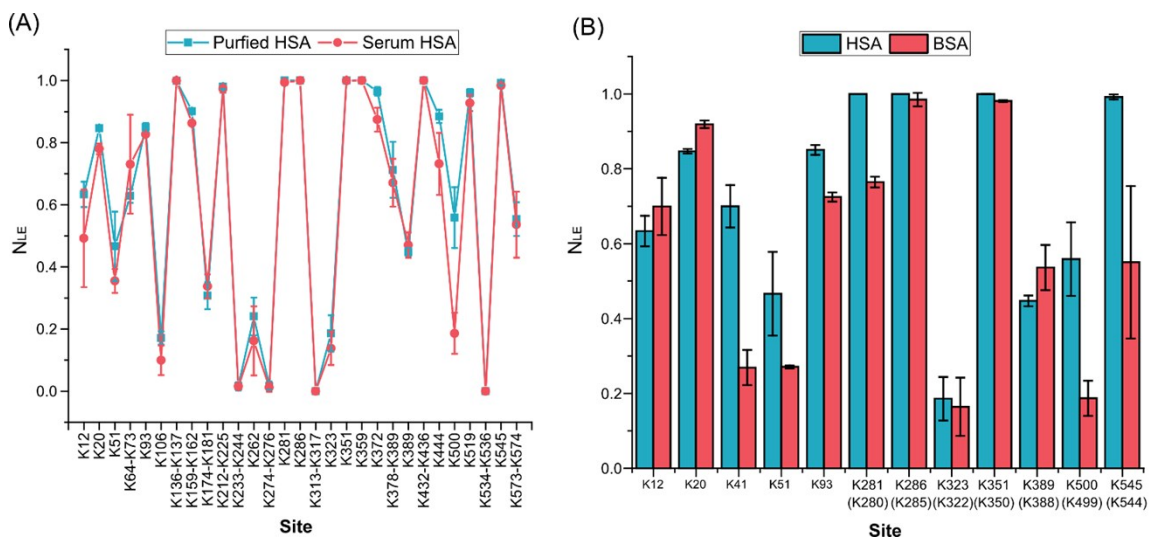


Fig. S3. Quantification of the relative lysine reactivity of HSA by TILLRP strategy. **(A)** The N_{LE} profiles of purified and serum HSA; **(B)** Comparison of the N_{LE} of conserved lysines in HSA and BSA, the lysines in brackets for BSA.

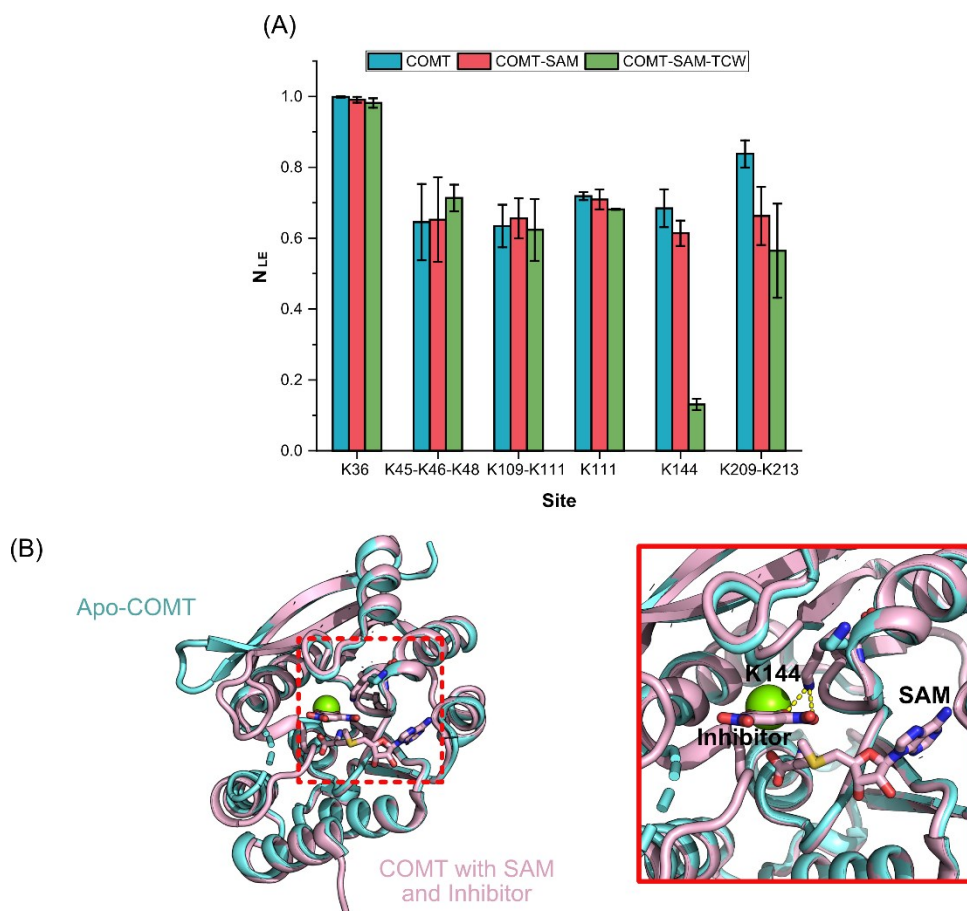


Fig. S4. Quantification of the lysine reactivity of COMT with/without ligand combination by TILLRP strategy. **(A)** comparison of the N_{LE} of lysine residues in COMT, COMT-SAM,

and COMT-SAM-TCW; **(B)** the microenvironments of Lys¹⁴⁴ in the crystal structure of apo-COMT (PDB: 4pyi) and COMT with ligands (PDB: 3bwy).

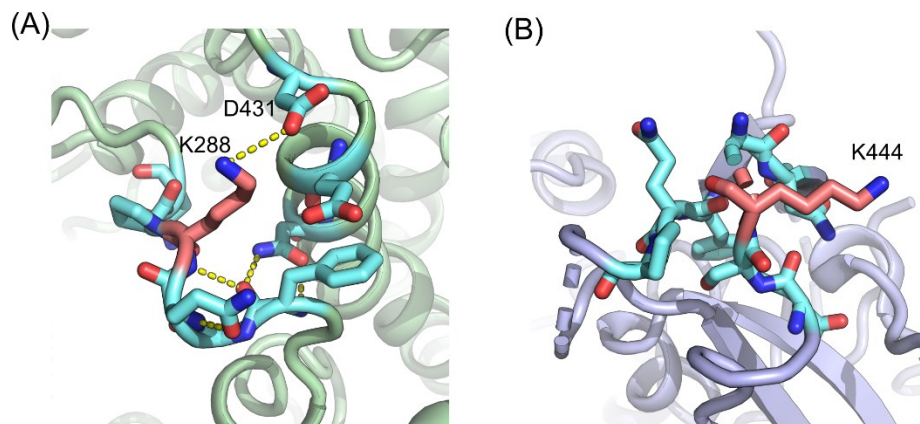


Fig. S5. The microenvironments of (A) ACE2 Lys²⁸⁸ (PDB: 6m18) and (B) S1 Lys⁴⁴⁴ (PDB: 6vxx). The salt bridge of lysine is shown as a yellow dashed line.

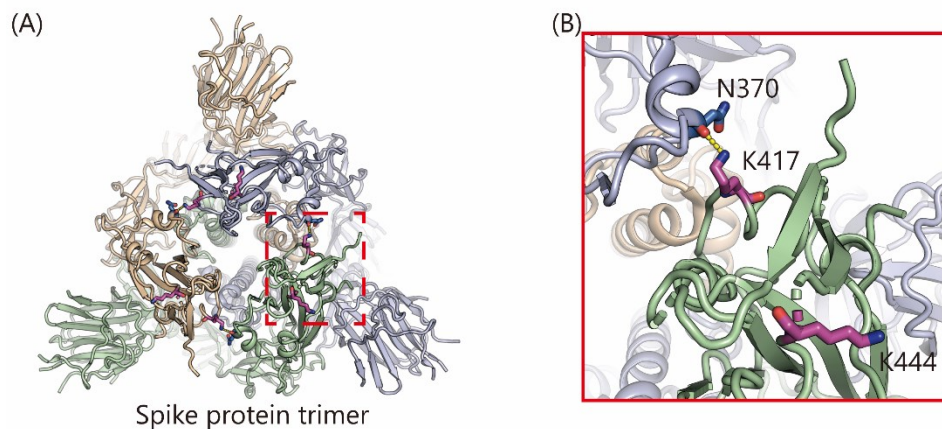


Fig. S6. The microenvironments of Lys⁴¹⁷ and Lys⁴⁴⁴ at the closed trimer Spike glycoprotein conformation (PDB: 6vxx). The salt bridge of lysine is shown as a yellow dashed line.

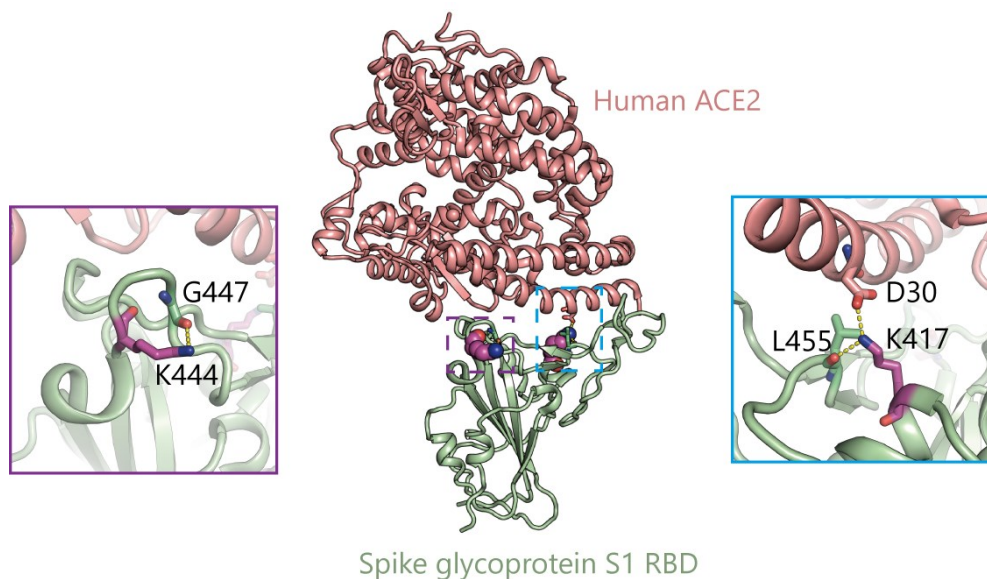


Fig. S7. The microenvironments of Lys⁴¹⁷ and Lys⁴⁴⁴ in SARS-CoV-2 S1-ACE2 complex (PDB: 6lzg). The salt bridge of lysines are shown as yellow dashed lines.

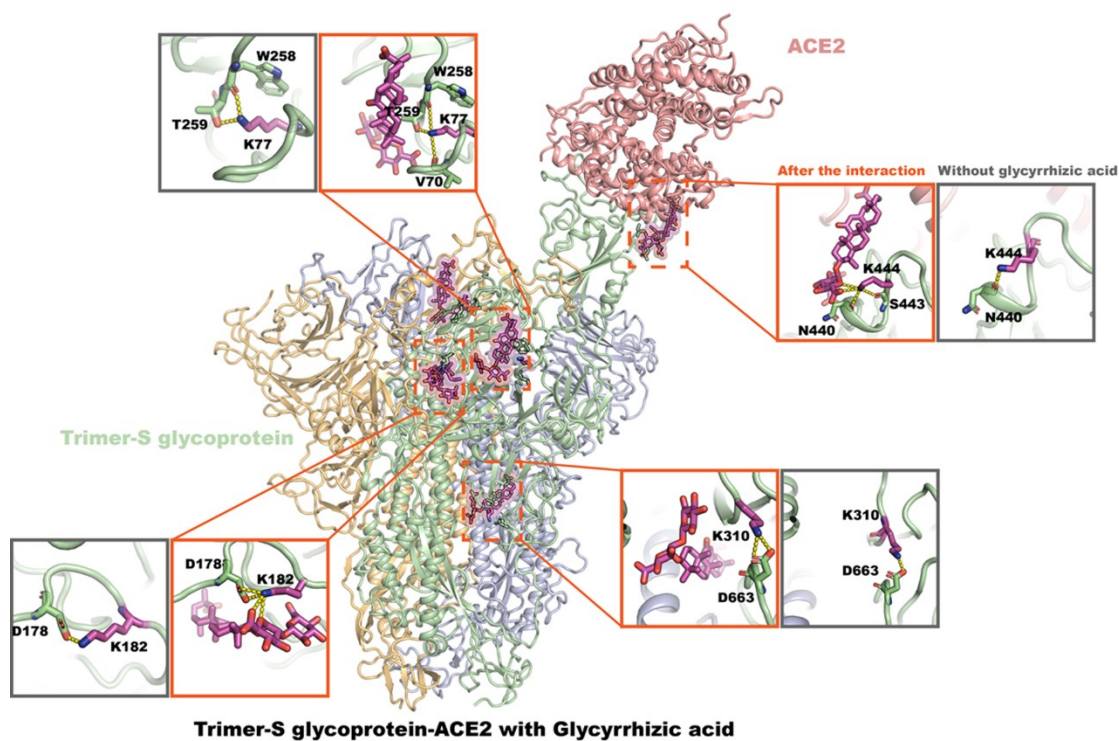


Fig. S8. Simulated docking conformation of the interactions of SARS-CoV-2 S1-ACE2 complex with glycyrrhizic acid. The gray and orange boxes represent the schematic diagram of lysine microenvironments before and after docking glycyrrhizic acid with S1-ACE2 complex. The salt bridges of lysines are shown as yellow dashed lines.

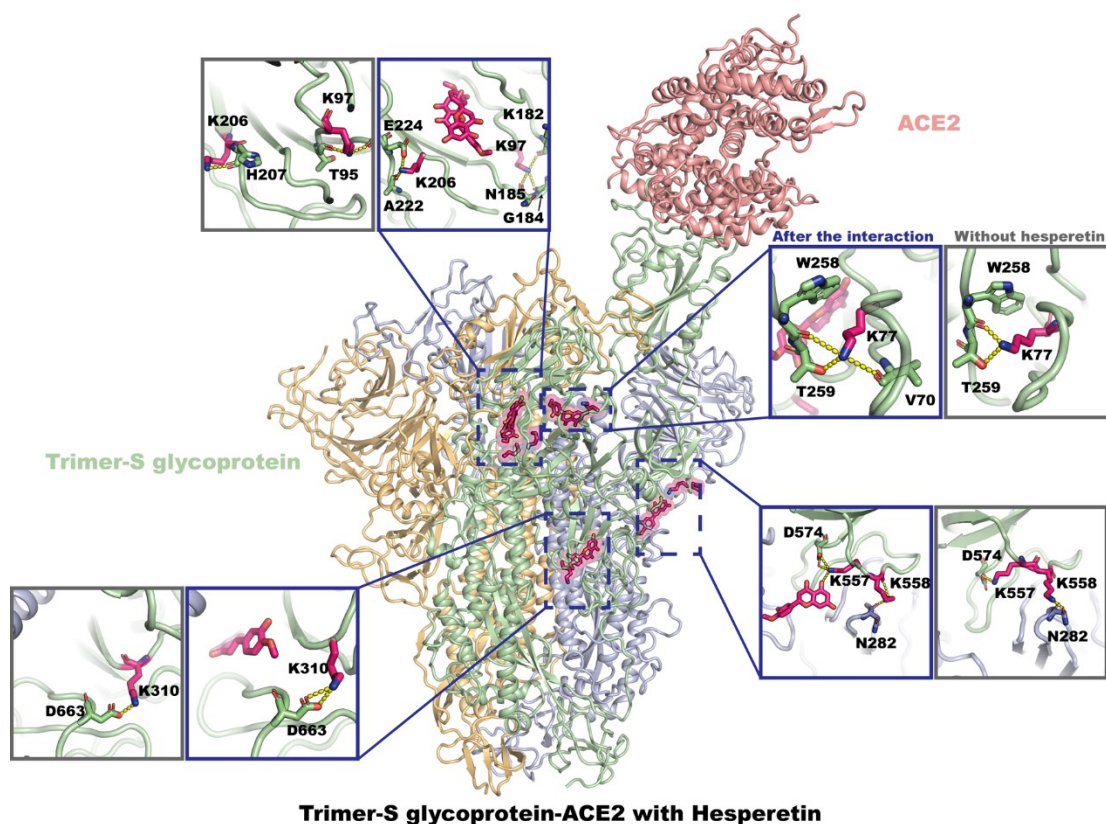


Fig. S9. Simulated docking conformation of the interactions of S1-ACE2 complex with hesperetin. The gray and blue boxes represent the schematic diagram of lysine microenvironments before and after docking hesperetin with S1-ACE2 complex. The salt bridges of lysines are shown as yellow dashed lines.

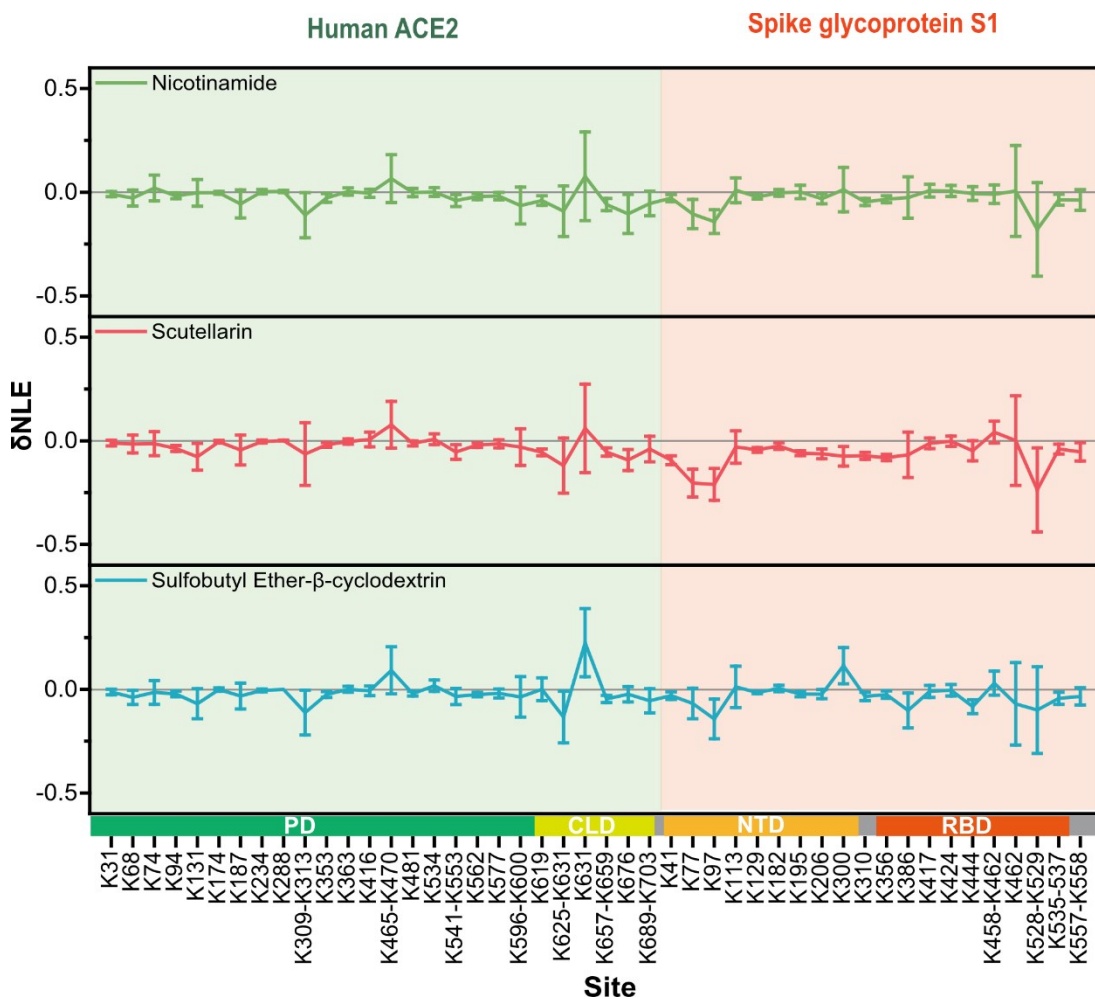


Fig. S10. The δN_{LE} of lysine residues in S1-ACE2 complexes modulated by the treatment of exogenous compounds nicotinamide, scutellarin, and sulfobutyl ether- β -cyclodextrin.